



Spatial nonlinearity in anisotropic metamaterial plasmonic slot waveguides

Mahmoud M. R. Elsawy, Gilles Renversez

► To cite this version:

Mahmoud M. R. Elsawy, Gilles Renversez. Spatial nonlinearity in anisotropic metamaterial plasmonic slot waveguides. 2016. hal-01360397

HAL Id: hal-01360397

<https://amu.hal.science/hal-01360397>

Preprint submitted on 6 Sep 2016

HAL is a multi-disciplinary open access archive for the deposit and dissemination of scientific research documents, whether they are published or not. The documents may come from teaching and research institutions in France or abroad, or from public or private research centers.

L'archive ouverte pluridisciplinaire **HAL**, est destinée au dépôt et à la diffusion de documents scientifiques de niveau recherche, publiés ou non, émanant des établissements d'enseignement et de recherche français ou étrangers, des laboratoires publics ou privés.

Spatial nonlinearity in anisotropic metamaterial plasmonic slot waveguides

MAHMOUD M. R. ELSAWY¹ AND GILLES RENVERSEZ^{1,*}

¹Aix-Marseille Univ, CNRS, Ecole Centrale Marseille, Institut Fresnel, 13013 Marseille, France

*Corresponding author: gilles.renversez@univ-amu.fr

Compiled September 5, 2016

We study the main nonlinear solutions of plasmonic slot waveguides made from an anisotropic metamaterial core with a positive Kerr-type nonlinearity surrounded by two semi-infinite metal regions. First, we demonstrate that for a highly anisotropic diagonal elliptical core, the bifurcation threshold of the asymmetric mode is reduced from GW/m threshold for the isotropic case to 50 MW/m one indicating a strong enhancement of the spatial nonlinear effects, and that the slope of the dispersion curve of the asymmetric mode stays positive, at least near the bifurcation, suggesting a stable mode. Second, we show that for the hyperbolic case there is no physically meaningful asymmetric mode, and that the sign of the effective nonlinearity can become negative.

OCIS codes: (240.6680) Surface plasmons, (230.7390) Waveguides, planar, (190.6135) Spatial solitons, (190.3270) Kerr effect, (160.3918) Metamaterials

Nonlinear plasmonics is now a thriving research field [1]. Among it, its integrated branch where surface plasmon polariton waves propagates at least partially in nonlinear media is seen as promising in high-speed small footprint signal processing. As a building block for nonlinear plasmonic circuitry, the nonlinear plasmonic slot waveguide (NPSW) is of crucial importance even in its simplest version [2, 3]. Since all the key features can be studied and understood in detail, this structure allows us future generalizations from more complex linear structures like the hybrid plasmonic waveguide [4]. The strong field confinement achieved by these plasmonic waveguides ensure a reinforcement of the nonlinear effects which can be boosted further using epsilon-near-zero (ENZ) materials as it was already shown [5, 6]. It is worth mentioning that metal nonlinearities have already been investigated including at least in one study where the wavelength range of enhanced nonlinearity has been controlled using metamaterials [7]. Here, we focus on structures where the nonlinearity is provided by dielectric materials like hydrogenated amorphous silicon (a-Si:H) [8] due to its high intrinsic third order nonlinearity around the telecommunication wavelength and to its manufacturing capabilities.

In [5], nonlinear guided waves were investigated in anisotropic structures with an isotropic effective dielectric re-

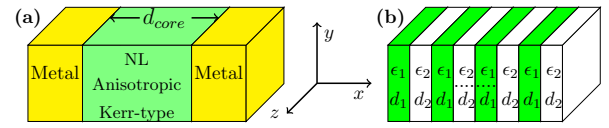


Fig. 1. (a) Symmetric NPSW geometry with its metamaterial nonlinear core and the two semi-infinite metal regions. (b) Metamaterial nonlinear core obtained from a stack of two types of layers with permittivities and thicknesses ϵ_1 and d_1 , and ϵ_2 and d_2 , respectively. Only material 1 is nonlinear.

sponse for transverse magnetic (TM) waves while here we consider a metamaterial core with an anisotropic effective dielectric response for TM waves. Other related works [6, 7] did not focus on the nonlinear waveguide problem or did not consider plasmonic structures. This task will be realized in the present study. Furthermore, in indium tin oxide layer, a record change of 0.72 in the refractive index increase induced by a third order nonlinearity has recently been reported [9]. As concluded by the authors, this result challenges the usual hypothesis that the nonlinear term can be treated as a perturbation. One approach to tackle this problem, for the case of nonlinear stationary waves, is to take into account the spatial profile of the fields directly from Maxwell's equations as for example in [10, 11]. To start by this case is justified because in waveguide studies whatever they are linear or nonlinear, it is well established that the modal approach is the first key step [12] requiring to investigate the self-coherent stationary states of Maxwell's equations. Here, extending methods we developed to study stationary states in isotropic NPSWs [13, 14] to the anisotropic case, we describe the main properties obtained when a nonlinear metamaterial is used as core medium. The examples of metamaterial nonlinear cores used in the following are built using effective medium theory from well-known materials and realistic parameters. The main nonlinear solutions in both elliptical and hyperbolic cases are investigated. In the first case, we demonstrate numerically and theoretically that for a highly anisotropic case, the effective nonlinearity [13] can be enhanced nearly up to five orders of magnitude allowing a decrease of nearly three orders of magnitude of the bifurcation threshold of the asymmetric mode existing in the symmetric structure [3, 14]. Next, we show that, in the hyperbolic case, changes appear in the field profiles com-

pared to the simple isotropic NPSWs. We also demonstrate that due to the peculiar anisotropy, an effective defocusing effect can be obtained from the initial positive Kerr nonlinearity.

Figure 1 shows a scheme of the nonlinear waveguide we investigate. Compared to already studied NPSW with an isotropic nonlinear dielectric core [2, 3, 15], the new structure contains a metamaterial nonlinear core. We will study only symmetric structures even if asymmetric isotropic NPSWs have already been considered [14]. We consider monochromatic TM waves propagating along the z direction (all field components evolve proportionally to $\exp[i(k_0 n_{eff} z - \omega t)]$ in a one-dimensional NPSW depicted in Fig. 1. Here $k_0 = \omega/c$, where c denotes the speed of light in vacuum, n_{eff} denotes the effective mode index and ω is the light angular frequency. The electric field components are $(E_x, 0, iE_z)$ and the magnetic field one is $(0, H_y, 0)$. In all the waveguide, the magnetic permeability is equal to μ_0 , the one of vacuum.

The nonlinear Kerr-type metamaterial core of thickness d_{core} is anisotropic (see Fig. 1). Its full effective permittivity tensor $\bar{\epsilon}_{eff}$ has only three non-null diagonal terms. Its linear diagonal elements are $\epsilon_{jj} \forall j \in \{x, y, z\}$. We derive these terms from simple effective medium theory (EMT) applied to a stack of two isotropic material layers. d_1 and d_2 are the layer thicknesses of isotropic material 1 (nonlinear focusing Kerr-type) and material 2 (linear), respectively. Their respective linear permittivities are ϵ_1 and ϵ_2 . The EMT is typically valid when the light wavelength λ is much larger than d_1 and d_2 . Depending on the chosen orientation of the compound layers relative to the Cartesian coordinate axes, different anisotropic permittivity tensors can be build for the core. Due to the required z -invariance, only two types where the z -axis belongs to the layers have to be considered. For the first one where the layers are parallel to the x -axis, one has, for the linear diagonal terms of $\bar{\epsilon}_{eff}$: $[\epsilon_{xx} = \epsilon_{yy} = \epsilon_{\perp} \quad \epsilon_{zz} = \epsilon_{//}]$ with $\epsilon_{//} = \Re(re_2 + (1-r)\epsilon_1)$, $\epsilon_{\perp} = \Re((\epsilon_1\epsilon_2)/(\epsilon_1 + (1-r)\epsilon_2))$, and $r = d_2/(d_1 + d_2)$. For the second case where the layers are parallel to the y -axis (see Fig. 1 (b)), one gets: $[\epsilon_{\perp} \quad \epsilon_{//} \quad \epsilon_{//}]$. We will focus only on this case.

To model these anisotropic waveguides, we assume that the nonlinear Kerr term is isotropic. This is an approximation compared to the full treatment [16, 17]. To tackle the full case is beyond the scope of our study which is mostly dedicated to the impact of the anisotropy of the linear terms even if its extension can be seen as the next required step in this research field. In this study, the wavelength is $1.55 \mu\text{m}$. ϵ_1 (corresponding to a-Si:H), and metal (gold) permittivity are the same as in [18], while d_{core} is fixed to 400nm (except in Fig. 2), and the nonlinear coefficient for the first material denoted by $n_{2,1}$ is set to $2.10^{-17} \text{m}^2/\text{W}$. Next, the two used models of the Kerr nonlinear field dependency are described.

In the first one, only the transverse component of the electric field E_x which is usually larger than the longitudinal one is taken into account. This approximation has already been used in several models of isotropic NPSWs [13, 15, 18]. It gives similar results than more accurate approaches where all the electric field components are considered in the optical Kerr effect [13, 15]. This first model allows us to use our new semi-analytical approach called EJEM (for Extended Jacobi Elliptical Model which is an extension to the anisotropic case [17] of our already developed JEM valid for isotropic configurations [13]). This approach will provide insights into the dependency of the effective nonlinearity on the opto-geometrical parameters. This approximation for the nonlinear term also allows us to use the simple fixed

power algorithm in the finite element method (FEM) to compute the nonlinear stationary solutions and their nonlinear dispersion curves [11, 19–21] in order to validate our EJEM results.

In the second model, all the electric field components are considered in the nonlinear term, and we need to use the more general FEM approach we developed [17] to generalize the one-component fixed power algorithm [15] in such structures.

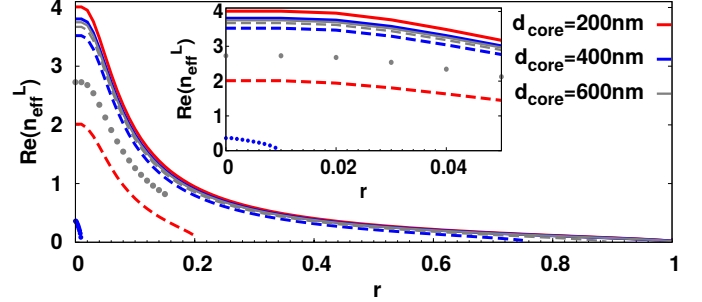


Fig. 2. Linear dispersion curves for symmetric NPSWs as a function of r parameter in the elliptical case for three different core thicknesses d_{core} with $\epsilon_2 = 1.0 \cdot 10^{-5} + i0.62$. Solid lines stand for first symmetric modes, dashed lines for first anti-symmetric modes, and points for first higher-order symmetric modes. Inset: zoom for the region near $r = 0$.

Now, we investigate the elliptical case for the metamaterial nonlinear core NPSWs. We choose for material 2 in the core an ENZ-like one such that $\epsilon_2 = 1.0 \cdot 10^{-5} + i0.62$ being similar to the one provided in [22]. We start this study by the linear case in which the main linear modes we found are of plasmonic type. For the metamaterial core, besides the permittivities, we have the ratio r defined above as new degree of freedom. As a result, one can obtain linear dispersion curves as a function of r . Fig. 2 shows such curves for several values of the core thickness d_{core} . n_{eff}^L indicates n_{eff} of the linear case. One can see that it is possible to choose configurations where only the first symmetric mode is kept. This kind of behaviour can be an advantage to reach a simpler and better control of nonlinear propagating solutions as a function of power [23] or to tune the linear dispersion properties as a function of wavelength to manage the dispersion coefficients.

As a test signature for strong nonlinear spatial behaviour and a demanding validity check, we depict the Hopf bifurcation of symmetric mode toward an asymmetric mode in symmetric isotropic and anisotropic NPSWs. In Fig. 3, we provide the results obtained with the methods we used, the EJEM one and the two FEM ones with and without all the electric field components in the nonlinear term. For comparison with this last case, we also use the interface model (IM) we developed previously to study the isotropic case taking into account all the electric field components [13]. First for the isotropic case (Fig. 3 (a)), the FEM taking account only the electric field transverse component is able to recover the results from the EJEM, and our FEM with both electric field components reproduces the results obtained from the IM. Second, for the anisotropic case (Fig. 3 (b)), the EJEM and FEM agrees well. As expected, the results between FEM with and without all the electric field components in the nonlinear term differ slightly at high powers. Consequently, these results prove the validity of our numerical methods for nonlinear studies including the anisotropic case.

Despite, the enhancement of nonlinear effects due to the use

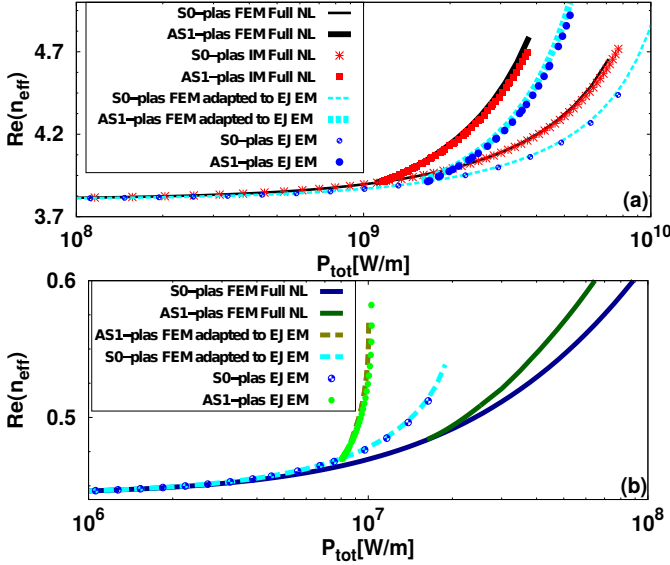


Fig. 3. Nonlinear dispersion curves for symmetric NPSWs as a function of total power P_{tot} . Both the symmetric modes (bottom branch for each color) denoted S0-plas and the asymmetric ones AS1-plas (upper branch after bifurcation) are shown, the mode notation is fully coherent with the ones used for the simple [13, 14] or improved [18] isotropic NPSWs. (a) Isotropic case with the EJEM, the FEM with and without all the electric field components in the nonlinear term, and the IM. (b) Elliptical anisotropic case with the EJEM, and the two FEMs.

of ENZ materials demonstrated both theoretically [5–7] and experimentally [9], Fig. 4 shows that, in the isotropic case, the ENZ material core does not reduce the bifurcation threshold but increases it. This can be understood qualitatively as follows. In ENZ material the wavelength light is stretched thus the two core interfaces are then more tightly coupled and more power is needed by the nonlinearity to break the symmetry of the field profile.

In the anisotropic case, as it can be seen in Figs. 3 (b) and 5, to consider a nonlinear core with ENZ ϵ_{xx} and large ϵ_{zz} allows us to drastically reduce the needed total power to induce the symmetry breaking in the NPSW compared to the usual isotropic case. As a result, we can shift from a GW/m threshold to approximately 50 MW/m one. Using our semi-analytical EJEM,

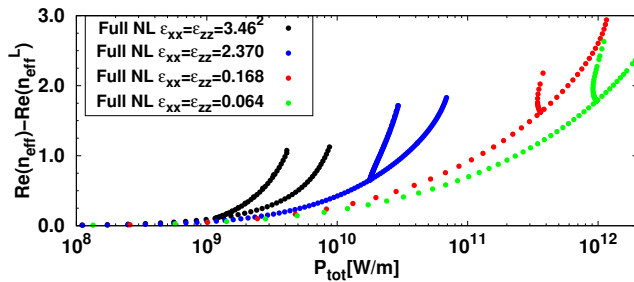


Fig. 4. Nonlinear dispersion curves for isotropic symmetric NPSWs as a function of total power P_{tot} and for different values of linear core permittivity. Both the symmetric modes and the asymmetric ones are shown.

we obtain the following analytical expression for the effective nonlinearity term [13] in the studied anisotropic NPSWs [17]:

$$a_{nl}^{EJEM} = -\tilde{\alpha} n_{eff}^2 \left(n_{eff}^2 (\epsilon_{xx} - \epsilon_{zz}) - \epsilon_{xx}^2 \right) / \left(\epsilon_{xx}^4 c^2 \epsilon_0^2 \right) \quad (1)$$

with $\tilde{\alpha} = \epsilon_0 c \Re(\epsilon_1)(1-r)n_{2,1}$. Consequently, for the NPSWs, the reinforcement of the effective nonlinearity when ENZ ϵ_{xx} and large ϵ_{zz} is clearly understood and quantified. It seems to have been partially overlooked in some previous studies due to the fact that most attention was dedicated to the permittivity tensor case one [$\epsilon_{//} \ \epsilon_{\perp} \ \epsilon_{//}$] leading to $\epsilon_{xx} = \epsilon_{zz} = \epsilon_{//}$, and not the case two as studied here with [$\epsilon_{\perp} \ \epsilon_{//} \ \epsilon_{//}$] leading to non-vanishing terms in Eq. (1). The observed reduction of the bi-

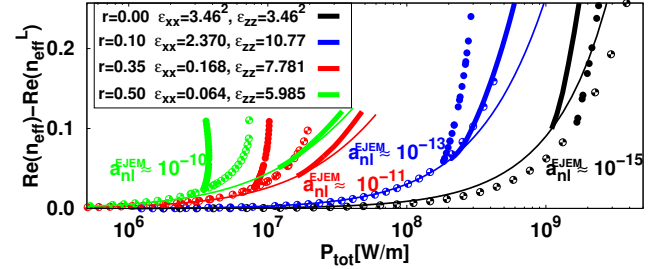


Fig. 5. Nonlinear dispersion curves for elliptical anisotropic and isotropic symmetric NPSWs as a function of total power P_{tot} for different values of the ratio r . Both the symmetric modes and the asymmetric ones are shown. The curves have been translated along the y -axis to improve visibility. The associated values of the effective nonlinearity a_{nl}^{EJEM} at the bifurcation threshold are also given.

furcation threshold is not possible neither in isotropic improved NPSWs [18] nor in isotropic ENZ NPSWs as shown in Fig. 4. Fig. 6 gives the thresholds as a function of transverse and longitudinal permittivities for several configurations. Above the black line associated to the isotropic case, one gets higher thresholds while they are smaller below. In the anisotropic case, for ENZ ϵ_{xx} , one can see the strong decrease of the threshold. For a fixed ϵ_{xx} , an increase of ϵ_{zz} induces a decrease of the bifurcation threshold (see inset in Fig. 6). Nevertheless, it can be argued that order of magnitude threshold decreases have already been predicted [13, 14] but this result was obtained using a large increase of the core size moving the structure from nanophotonics to large integrated optics structures. In the present case, small core thicknesses can be kept allowing not only a limited footprint for the devices but also a limited number of propagating modes in the metamaterial based NPSWs, eventually only the fundamental symmetric mode (see Fig. 2) and the associated asymmetric one. One can also notice that the slopes of the symmetric mode nonlinear dispersion curves for the studied highly anisotropic NPSWs are not negligible even below the reduced bifurcation threshold involving important nonlinear effects on the propagation of this mode even at lower powers. Another consequence of the use of a highly anisotropic elliptical metamaterial core is the low value of the effective indices for the main modes (see Fig. 3 (b)) ensuring a slow light enhancement for the nonlinear effects in temporal propagation configurations [24]. The impact of the core anisotropy is also seen on the dispersion curve of the main asymmetric mode. As shown, in Fig. 4 (isotropic case), the lower the index core permittivity, the larger the slope of the

asymmetric mode branch. Moreover, for ENZ isotropic core ($\epsilon_{core} \lesssim 1$), the slope is negative while, as shown in Fig. 5, for highly anisotropic core with ENZ ϵ_{xx} and large ϵ_{zz} , the slope of the asymmetric mode near the bifurcation point stays positive. If we assume that the stability results we obtained for isotropic NPSWs [14] can be extended to the anisotropic case, these two features suggest that the asymmetric mode should be unstable in isotropic ENZ core NPSWs ($\epsilon_{core} \lesssim 1$) while the same mode should be stable for highly anisotropic core with ENZ ϵ_{xx} and large ϵ_{zz} (a full stability study of the main modes as described in [14] for simple NPSWs is beyond the scope of this work).

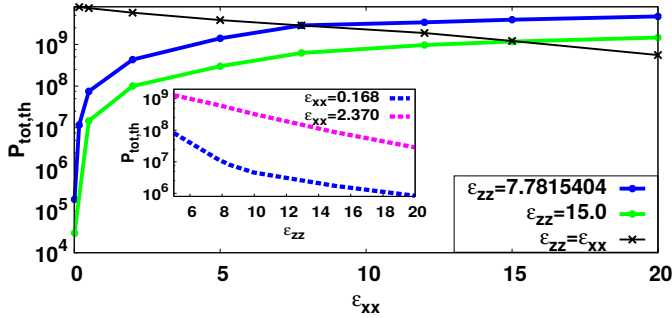


Fig. 6. Power threshold $P_{tot,th}$ as a function of linear transverse permittivity ϵ_{xx} in the elliptical case for two longitudinal permittivity ϵ_{zz} values. Isotropic case is shown by the black curve. Inset: $P_{tot,th}$ as a function of ϵ_{zz} for two ϵ_{xx} values.

We now investigate the hyperbolic case where the metamaterial core is such that $\epsilon_{xx} > 0$ and $\epsilon_{zz} < 0$. In this case, it is known that non-local effects can be neglected in EMT as soon as the condition $d_1 = d_2$ is fulfilled corresponding to $r = 0.5$ [25]. We will limit the study to such configurations. Linear studies of waveguides involving such linear metamaterial core have already been published [26]. For NPSWs, we found that the main modes are core localized unlike the ones of simple NPSWs, and that the effective nonlinearity can be negative for the investigated modes meaning that the initial positive Kerr nonlinearity can finally act as a negative one in such anisotropic configuration. This can be understood looking at Eq. (1). Fig. 7 (a) illustrates this phenomenon. We also found that the asymmetric mode we can obtain as a mathematical solution of the nonlinear dispersion equation is actually unbounded [17], knowing that similar unbounded modes were already obtained in other nonlinear structures [27]. Therefore, this asymmetric mode can not be considered as an acceptable solution of our physical problem. The nonlinear dispersion curves of the main symmetric and antisymmetric modes are given in Fig. 7 (b). Once again, one can see the crucial influence of the metamaterial core properties on the type and behaviour of the propagating nonlinear solutions.

The found spatial nonlinear effects are a signature of a strong nonlinear reinforcement. We move from a GW/m bifurcation threshold required in the isotropic cases [14] even in improved NPSWs [18] to tens of MW/m one for elliptical anisotropic NPSWs with ENZ ϵ_{xx} and large ϵ_{zz} . This improvement makes the properties of the proposed waveguides really achievable to materials used in current fabrication processes in photonics and also to most characterization setups.

Acknowledgments. G. R. would like to thank the PhD school ED 352 "Physique et Sciences de Matière" and the International Relation Service of Aix-Marseille University (project AAP 2015 "Noliplasma 2D") for their respective fundings.

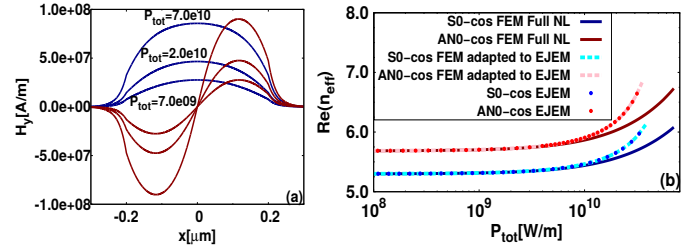


Fig. 7. Hyperbolic symmetric NPSWs for $\epsilon_{xx} = 26.716$ and $\epsilon_{zz} = -51.514$ (obtained from material 2 permittivity $\epsilon_2 = -115 + i6$ (copper) and $r = 0.5$). (a) Field profile $H_y(x)$ as a function of total power P_{tot} . (b) Nonlinear dispersion curves as a function of P_{tot} . The main symmetric and antisymmetric modes are shown for both the EJEM and the two FEM.

REFERENCES

1. M. Kauranen and A. V. Zayats, "Nonlinear plasmonics," *Nature Photon.* **6**, 737–748 (2012).
2. E. Feigenbaum and M. Orenstein, "Plasmon-soliton," *Opt. Lett.* **32**, 674–676 (2007).
3. A. R. Davoyan, I. V. Shadrivov, and Y. S. Kivshar, "Nonlinear plasmonic slot waveguide," *Opt. Express* **16**, 21209–21214 (2008).
4. R. F. Oulton, V. J. Sorger, D. A. Genov, D. F. P. Pilei, and X. Zhang, "A hybrid plasmonic waveguide for subwavelength confinement and long-range propagation," *Nature Photonics* **2**, 496–500 (2008).
5. A. Ciattoni, C. Rizza, and E. Palange, "Extreme nonlinear electrodynamics in metamaterials with very small linear dielectric permittivity," *Phys. Rev. A* **81**, 043839 (2010).
6. A. Ciattoni, C. Rizza, A. Marini, A. Di Falco, D. Faccio, and M. Scalora, "Enhanced nonlinear effects in pulse propagation through epsilon-near-zero media," *Laser & Photonics Reviews* **10**, 517–525 (2016).
7. A. D. Neira, N. Olivier, M. E. Nasir, W. Dickson, G. A. Wurtz, and A. V. Zayats, "Eliminating material constraints for nonlinearity with plasmonic metamaterials," *Nat Commun.* **6**, 7757 (2015).
8. C. Lacava, P. Minzioni, E. Baldini, L. Tartara, J. M. Fedeli, and I. Cristiani, "Nonlinear characterization of hydrogenated amorphous silicon waveguides and analysis of carrier dynamics," *Appl. Phys. Lett.* **103**, 141103 (2013).
9. M. Z. Alam, I. De Leon, and R. W. Boyd, "Large optical nonlinearity of indium tin oxide in its epsilon-near-zero region," *Science* **352**, 795–797 (2016).
10. A. W. Snyder, D. J. Mitchell, and Y. Chen, "Spatial solitons of Maxwell's equations," *Optics Letters* **19**, 524–526 (1994).
11. F. Drouart, G. Renversez, A. Nicolet, and C. Geuzaine, "Spatial Kerr solitons in optical fibres of finite size cross section: beyond the Townes soliton," *J. Opt. A: Pure Appl. Opt.* **10**, 125101 (2008).
12. A. W. Snyder, D. J. Mitchell, and L. Poladian, "Linear approach for approximating spatial solitons and nonlinear guided modes," *J. Opt. Soc. Am. B* **8**, 1618–1620 (1991).
13. W. Walasik and G. Renversez, "Plasmon-soliton waves in planar slot waveguides. I. modeling," *Phys. Rev. A* **93**, 013825 (2016).
14. W. Walasik, G. Renversez, and F. Ye, "Plasmon-soliton waves in planar slot waveguides. II. results for stationary waves and stability analysis," *Phys. Rev. A* **93**, 013826 (2016).
15. W. Walasik, A. Rodriguez, and G. Renversez, "Symmetric plasmonic slot waveguides with a nonlinear dielectric core: Bifurcations, size effects, and higher order modes," *Plasmonics* **10**, 33–38 (2015).
16. R. W. Boyd, *Nonlinear Optics* (Academic, New York, 2007).
17. M. M. R. Elsayy and G. Renversez, "Study of plasmonic slot waveguides with metamaterial nonlinear core: methods and results," to be submitted (2016).
18. M. M. R. Elsayy and G. Renversez, "Improved nonlinear slot waveguides using dielectric buffer layers: properties of TM waves," *Opt. Lett.* **41**, 1542–1545 (2016).
19. B. M. A. Rahman, J. R. Souza, and J. B. Davies, "Numerical analysis

- of nonlinear bistable optical waveguides," IEEE Photon. Technol. Lett. **2**, 265–267 (1990).
20. A. Ferrando, M. Zacarés, P. F. de Cordoba, D. Binosi, and J. A. Monso-riu, "Spatial soliton formation in photonic crystal fibers," Optics Express **11**, 452–459 (2003).
 21. W. Walasik, G. Renversez, and Y. V. Kartashov, "Stationary plasmon-soliton waves in metal-dielectric nonlinear planar structures: modeling and properties," Phys. Rev. A **89**, 023816 (2014).
 22. A. Capretti, Y. Wang, N. Engheta, and L. D. Negro, "Enhanced third-harmonic generation in si-compatible epsilon-near-zero indium tin oxide nanolayers," Opt. Lett. **40**, 1500–1503 (2015).
 23. N. N. Akhmediev and A. Ankiewicz, *Solitons, Nonlinear Pulses and Beams* (Chapman & Hall, London, 1997).
 24. T. Baba, "Slow light in photonic crystals," Nature Photonics **2**, 465 – 473 (2008).
 25. A. V. Chebykin, A. A. Orlov, A. V. Vozianova, S. I. Maslovski, Y. S. Kivshar, and P. A. Belov, "Nonlocal effective medium model for multilayered metal-dielectric metamaterials," Phys. Rev. B **84**, 115438 (2016).
 26. I. Avrutsky, I. Salakhutdinov, J. Elser, and V. Podolskiy, "Highly confined optical modes in nanoscale metal-dielectric multilayers," Phys. Rev. B **75**, 241402 (2007).
 27. W. Chen and A. A. Maradudin, "s-polarized guided and surface electromagnetic waves supported by a nonlinear dielectric film," J. Opt. Soc. Am. B **5**, 529–538 (1988).